Mechanistic insights into selective indium catalyzed coupling of epoxides and lactones

Kimia Hosseini,[1‡] *Chatura Goonesinghe,*[1‡] *Hootan Roshandel* [2] *Joseph Chang,*[1] *Kudzanai Nyamayaro,*[1] *Hyuk-Joon Jung,* [2] *Paula L. Diaconescu*[2*] *and Parisa Mehrkhodavandi*[1]*

[1] Department of Chemistry, University of British Columbia, 2036 Main Mall, Vancouver, British Columbia, V6T 1Z1, Canada

[2] Department of Chemistry and Biochemistry, University of California, Los Angeles, 607 Charles E. Young Drive East, Los Angeles, California 90095, United States

Abstract. Spiro-orthoesters, produced from the coupling of lactones and epoxides, are unique pre-sequenced monomers capable of producing alternating poly(ether-*alt*-ester) after ring opening polymerization. Recently, we reported the selective synthesis of spiro-orthoesters through the coupling of epoxides and lactones catalyzed by a cationic alkyl indium catalyst. Herein, we investigate the mechanism of this reaction using structure function relationships and computational studies. We show that this reaction is governed by Michaelis-Menten type saturation kinetics, which, along with the low Lewis acidity of these indium catalysts, explains their exceptional selectivity.

Introduction

Polymers with precisely controlled alternating monomer units have properties distinct from their homo-, block-, or gradient counterparts,[1,2] therefore, the sequence controlled synthesis of copolymers is challenging.[3-5] This has been particularly true in the synthesis of poly(ether-*alt*-esters) from epoxides and lactones; most attempts to create alternating copolymers form oligomers.[6-11] One successful method for producing alternating copolymers has been the polymerization of pre-sequenced monomers.[12-14] We are interested in spiro-orthoesters, which are capable of forming poly(ether-*alt*-esters) through double ring opening polymerization reactions.[15-17]

The synthesis of spiro-orthoesters has been dominated by the coupling of epoxides and lactones in the presence of Lewis or Brønsted acids (Figure 1a).[18-22] However, this method suffers from low selectivity due to the competing polymerization of the lactone and epoxide substrates. These side reactions often necessitate high temperature distillation for product isolation resulting in low yields (< 50%). While other selective synthetic procedures involving diazo precursors were reported by Coster and Lacour using rhodium and ruthenium catalysts, respectively,[23,24] the requirement for multi-step organic syntheses to produce precursors limits the scope and versatility of these methods.

a. Synthesis of spiro-orthoesters from acid-catalyzed coupling of epoxides and lactones

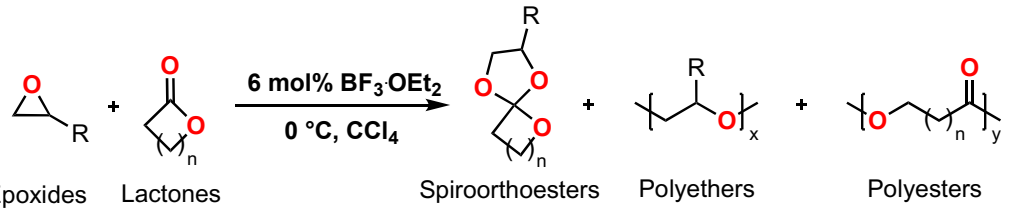

b. Proposed mechanism for the formation of spiro-orthoesters by Pascault and co-workers

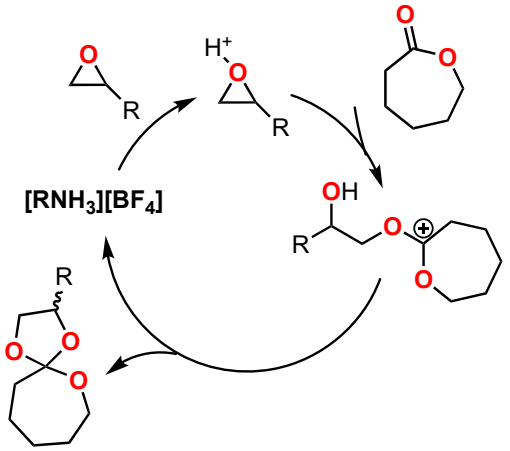

c. Temperature triggered. synthesis and polymerization of spiro-orthoesters

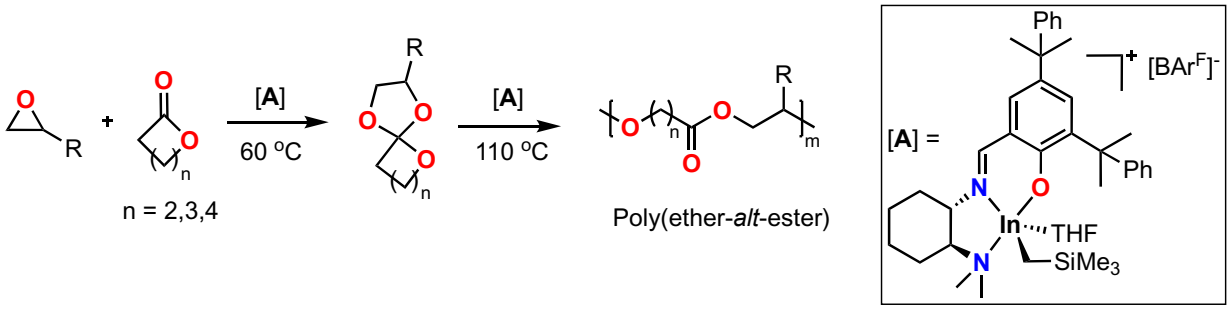

Figure 1. Prior studies in the coupling of epoxides and lactones.

Pascault and coworkers proposed a mechanism for the formation of spiro-orthoesters from lactones and epoxides that involves the activation of the epoxide *via* protonation with an acid, followed by attack of a lactone resulting in the ring opening of the epoxide (Figure 1b).[25] The final step was ring closure and release of the spiro-orthoester product. Although this hypothesis

rationalized the formation of spiro-orthoesters, the low selectivity of the reported systems has curtailed a detailed mechanistic examination of this reaction.

Recently, we reported that a cationic alkyl indium complex (Figure 1c, **A**) catalyzed the synthesis of a range of spiro-orthoesters from various epoxides and lactones with selectivity for coupling over polymerization reactions (Figure 1c).[26] Subsequently, we reported that **A** is capable of catalyzing the temperature-triggered double ring opening polymerization of spiro-orthoesters to yield alternating poly(ether-*alt*-ester) with the highest molecular weights reported to date (> 40,000 g/mol).[27]

In our work with cationic indium catalysts,[27,28] we have shown that their stability and reactivity can be significantly influenced by the addition of a hemilabile donor arm to the ligand backbone.[29,30] For example, adding a furfuryl pendant arm to **A** results in a catalyst with controlled activity and long shelf-life.[31] Herein, we elucidate the mechanism of spiro-orthoester formation using cationic indium complexes with hemilabile furfuryl pendant arms. We explore the structure-function relationship of different catalysts and demonstrate that the formation of spiro-orthoesters with these compounds is governed by Michaelis-Menten saturation kinetics.[32-34] To the best of our knowledge, this is the first detailed investigation of the mechanism of Lewis acid catalyzed formation of spiro-orthoesters from the coupling of epoxides and lactones and shows the value of using weak Lewis acidic catalysts in achieving selectivity.

Results and discussion

Synthesis of compounds. We hypothesized that the reactivity of **A** can be probed by tuning the In-alkyl group and by replacing the coordinated solvent (THF) with a donor arm that can be changed both sterically and electronically. The alkane elimination reaction of trialkyl indium

complexes (InR_3, R = CH_3, $CH_2CH(CH_3)_2$, $CH_2Si(CH_3)_3$) with proligands bearing a hemilabile furfuryl pendant group with various substituents in the α-furfuryl position (X = H, CH_3, Br) forms the neutral compounds **1a-e** (Scheme 1 , see SI for synthetic procedures). Reacting **1a-e** with $[PhNMe_2H][BAr^F]$ (BAr^F = tetrakis[3,5-bis(trifluoromethyl)phenyl]borate) forms the cationic species **2a-e**. Compounds **2a-c** will be used to probe the effect of the alkyl group, while **2d-e** will be used to probe the effect of the substituents on the pendant donor arms. Compound **2d** has a weakly electron donating methyl substituent at the α-position of the furan ring, while **2e** has a weakly electron withdrawing bromo group;[35,36] both substituents have similar steric bulk.[37,38] All new compounds were fully characterized (see SI). Additionally, the solid-state molecular structures of **1a** and **2e** were determined by single-crystal X-ray crystallography. In the solid state, the hemilabile pendant arm is coordinated to the cationic indium center in the absence of external donors (Figures 2 and S50).[31]

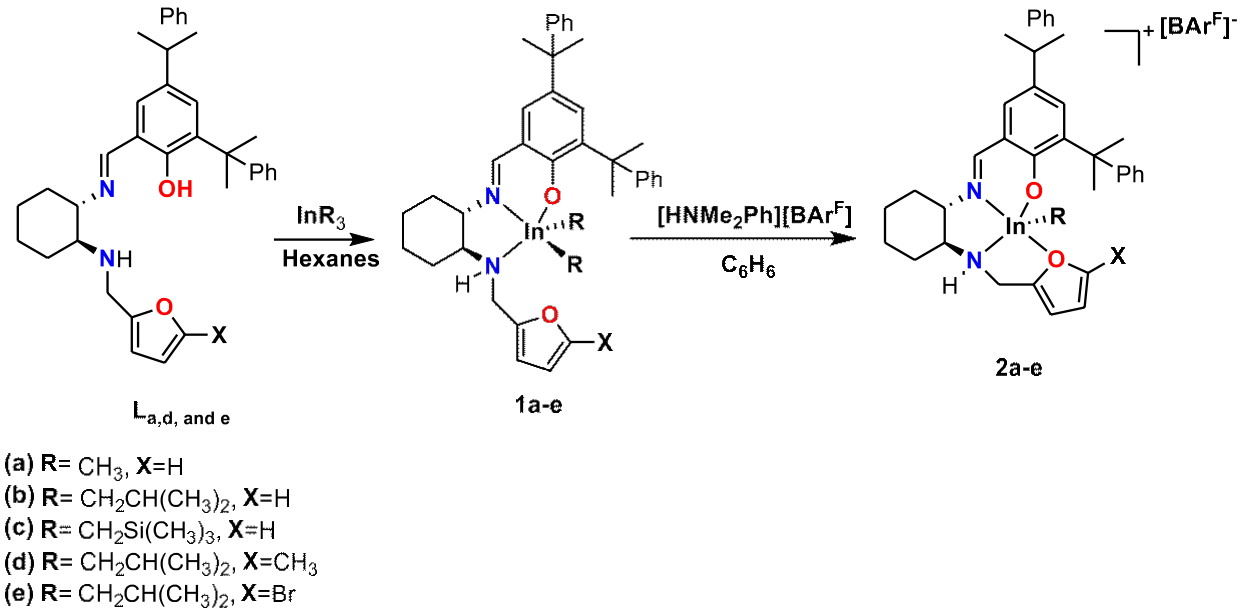

Scheme 1. Synthesis of neutral and cationic indium complexes.

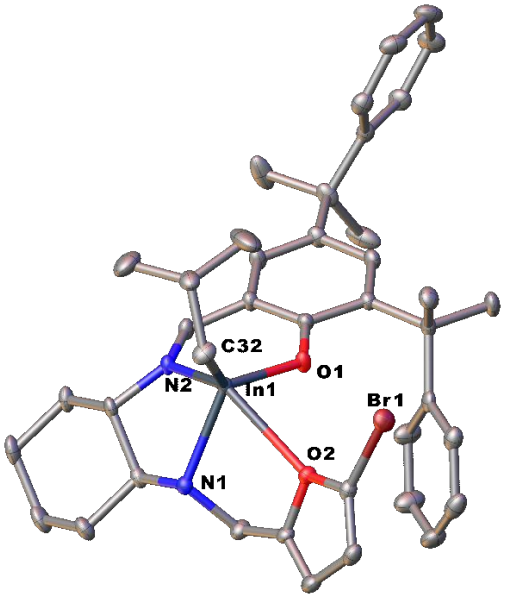

Figure 2. Molecular structure of **2e** depicted with thermal ellipsoids at 50% probability and H atoms, BAr^F counterion, solvent molecules, as well as minor disordered counterparts, omitted for clarity.

Evaluation of catalytic competency. We used **2a-e** as catalysts for the coupling of ε-caprolactone (**ε-CL**) and 1,2-epoxy-7-octene (**EOE**) to form 2-(hex-5-en-1-yl)-1,4,6-trioxaspiro[4.6]undecane (**SOE**) (Table 1). Compared to **A** (Figure 1c), **2a-e** exhibit slower conversions of **EOE** and higher stability, making them suitable catalysts to study the specific mechanism of this reaction. Monitoring SOE formation using **2b, 2d,** and **2e** as catalysts showed similar reactivity, demonstrating that the substituent on the α-position of the furfuryl pendant arm does not play a significant role in the mechanism of **SOE** formation (Figure S57).

Table 1. Synthesis of **SOE** from ε-caprolactone (**ε-CL**) and 1,2-epoxy-7-octene (**EOE**) using various cationic indium complexes.

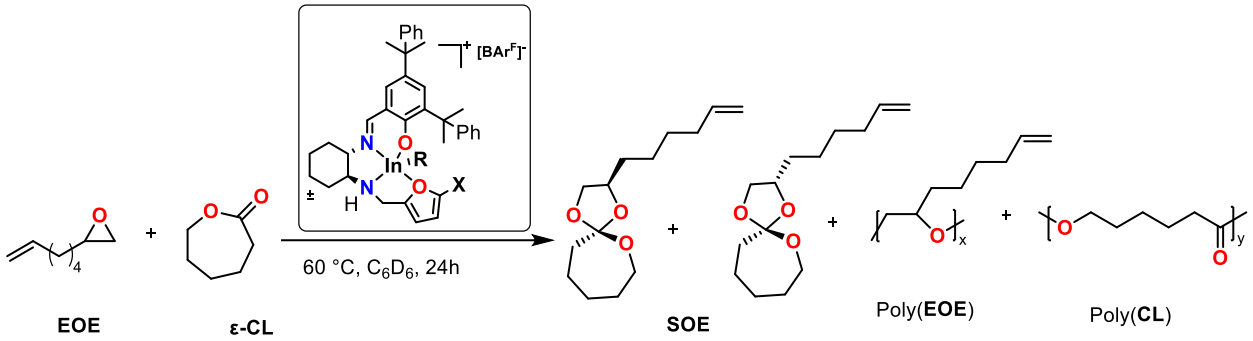

Entry	Catalyst	In-**R**	Furfuryl *α*-**X** group	Conversion of **EOE** (%) [b]	Poly(**EOE**) (%) [b]	Poly(**CL**) (%) [c]
1	**2a**	CH_3	H	48	<1	<1
2	**2b**	$CH_2CH(CH_3)_2$	H	55	<1	<1
3	**2c**	$CH_2Si(CH_3)_3$	H	78	<1	<1
4	**2d**	$CH_2CH(CH_3)_2$	CH_3	57	<1	<1
5	**2e**	$CH_2CH(CH_3)_2$	Br	60	<1	<1
6 [d]	**A**	$CH_2Si(CH_3)_3$	-	>99	<1	<1

[a] Reactions were performed in benzene for 24 h at 60 °C, [**EOE**] = [**ε-CL**] = 0.25 M, [catalyst] = 0.006 M. [b] Conversion was determined by ^{1}H NMR spectroscopy (400 MHz, C_6D_6, 25 ºC) and calculated with respect to **EOE**. [c] Determined by ^{1}H NMR spectroscopy (400 MHz, C_6D_6, 25 ºC). [d] Previously reported data for cationic indium complex **A**.[26]

Role of the alkyl ligands in determining reactivity. The total conversion of **EOE** and **ε-CL** to **SOE** at 24-hour reaction time increases in the following order **2a** < **2b** < **2c** (Table 1, entries 1-3). Correspondingly, **2a** has the slowest rate of conversion of epoxide to **SOE** monitored over 14 hours by ^{1}H NMR spectroscopy at 60 °C, followed by **2b**, with **2c** having the highest rate (Figure 3).

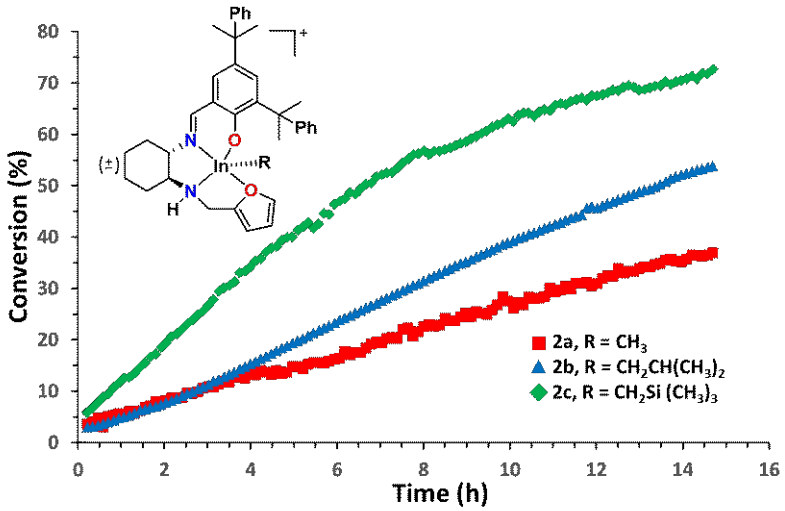

Figure 3. Conversion vs. time plots of **2a-c** for the formation of **SOE** monitored by ^{1}H NMR spectroscopy (60 °C, C_6D_6, 400 MHz).

Kinetics of spiro-orthoester formation. To identify the mechanism of **SOE** formation, we conducted kinetic analysis to determine the order of reaction with respect to **2b**, **EOE**, and **ε-CL**. The **SOE** formation was observed by *in situ* monitoring of the **SOE** proximal vinylic proton peak ($R(CH_2)_4CH{=}CH_2$)[26] using ^{1}H NMR spectroscopy at 60 °C. The concentrations of **2b**, **EOE**, or **ε-CL** were varied individually while the other components were kept constant. For each component, data from three different test concentrations were evaluated using variable time normalization analysis (VTNA).[39,40] The reaction profile was plotted against the time axis multiplied by Σ[**EOE**], Σ[**ε-CL**], or [**2b**] raised to different numerical power to visually overlap the plots (Figures 4 and S58-S60). Based on this analysis, the system shows first order rate dependence with respect to [**2b**]. However, changing either [**EOE**] or [**ε-CL**] has no effect on the rate of reaction and shows zeroth order with respect to both starting substrates. This points to catalyst saturation at these reaction conditions resulting in *pseudo*-zeroth order Michaelis-Menten type kinetics.[32-34]

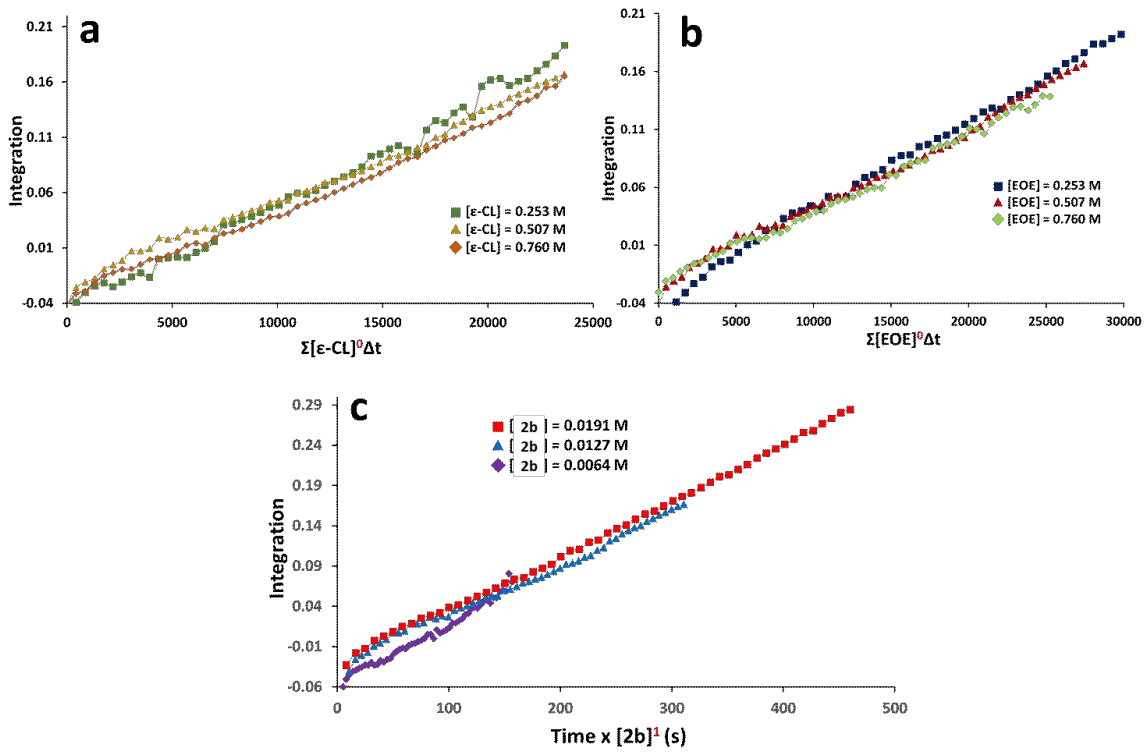

Figure 4. a) Variable time normalization analysis (VTNA) plot to determine the order with respect to [**ε-CL**]. ([**2b**] = 0.0127 M, [**EOE**] = 0.507 M at 60 °C in benzene-d_6). b) VTNA plot to determine the order with respect to [**EOE**] ([**2b**] = 0.0127 M, [**ε-CL**] = 0.507 M at 60 °C in benzene-d_6). c) VTNA plot to determine the order with respect to [**2b**] ([**EOE**] = 0.507 M, [**ε-CL**] = 0.507 M at 60 °C in benzene-d_6).

Michaelis-Menten kinetic analysis. In systems showing Michaelis-Menten kinetics, the rate of reaction is initially linearly dependent on the concentration of starting material; however, with increasing substrate concentration the rate approaches a maximum value for a given catalyst concentration.[34,41,42] The initial rate of **SOE** formation (M s^{-1}) increases when [**EOE**] and [**ε-CL**] are increased until the rate reaches a maximum value (V_{max}) indicating that the catalyst becomes kinetically saturated (Figure 5a). In enzyme kinetics, the Michaelis constant (K_M), i.e., the concentration of substrate at ½ V_{max}, is used as a measure of substrate affinity to a catalyst. Lower

K_M values correspond to stronger affinity, while higher values correspond to weaker affinity.[43] For biological enzymes, K_M values range from 10^{-1}-10^{-7} M, with the average enzyme showing K_M values of ~10^{-4} M.[44] Typical metal catalysts exhibiting saturation kinetics show K_M values in the range of 10^{-2}-10^{-4} M.[45] However for **2b** a Michaelis constant (K_M) of 0.43 M and a V_{max} of 6.43 M s^{-1} were calculated using the Eadie-Hofstee relationship (Figure 5b).[46] These values indicate that cationic alkylindium complexes have very low affinity to substrate at these reaction conditions, precluding the unwanted homopolymerization reactions of epoxides and lactones. This illustrates the importance of saturation kinetics in the selectivity of these catalysts.

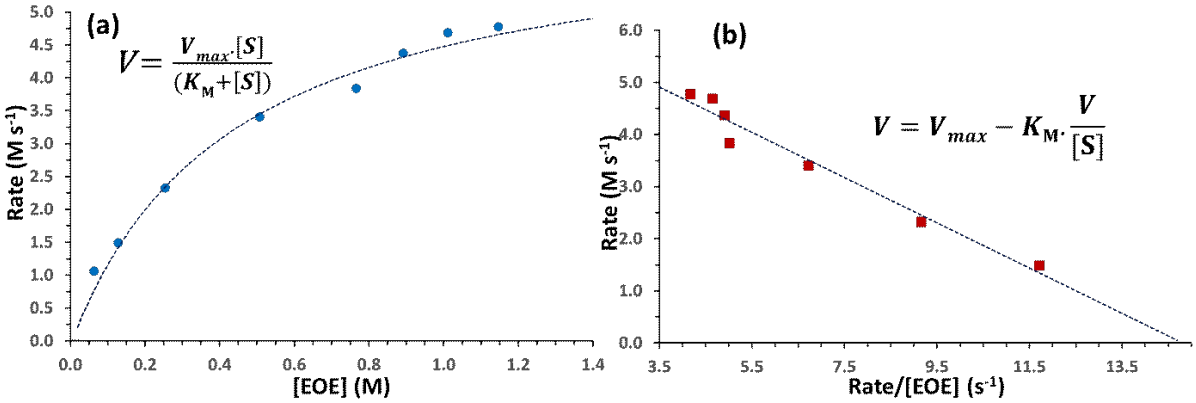

Figure 5. a) Saturation plot of **2b**. Line is plotted with K_M and V_{max} values extracted from the Eadie–Hofstee plot for **2b** (b).

Nature of the catalytically active species. Understanding the nature of the active catalytic species is a fundamental step in the elucidation of the mechanism of spiro-orthoester formation. Our previous studies with cationic alkyl indium complexes bearing hemilabile ligands have shown that the hemilability of the furfuryl pendant group has a significant effect on the reactivity of these compounds.[31] The change in the chemical shift of the α-proton of the furfuryl group in **2a-c** is an excellent determinant of the fluxionality of the donor arm. Using the difference in the chemical shift of this proton at 25 °C and chemical shifts at higher temperatures (Δδ), in variable temperature

(VT) ^{1}H NMR spectroscopy experiments, we show that **2a** has the lowest fluxionality followed by higher fluxionality in **2b** (Figures 6 and S52-S54). Compound **2c**, bearing the bulky $CH_2Si(CH_3)_3$ ligand, decomposes irreversibly at higher temperatures in the absence of external donor groups, showing significantly greater labile behavior than **2a** or **2b**. The more fluxional nature of the pendant arm results in higher reactivity of the cationic indium complexes in the formation of **SOE** with a reactivity order of **2a** < **2b** < **2c** (Table 1).

We aimed to investigate the correlation of the steric bulk of **2a-c**, quantified using %buried volume (%V_{bur}), to their temperature-dependent behavior (Figure S63).[47] The methyl ligand of **2a** contributes the lowest %V_{bur}, while **2b-c** have similar values. We postulate that the increased steric crowding leads to increased fluxionality of the furfuryl pendant arm. The difference in the relative stability of **2b** and **2c** arises from the electron withdrawing effects of the organosilicon ligand.[48,49]

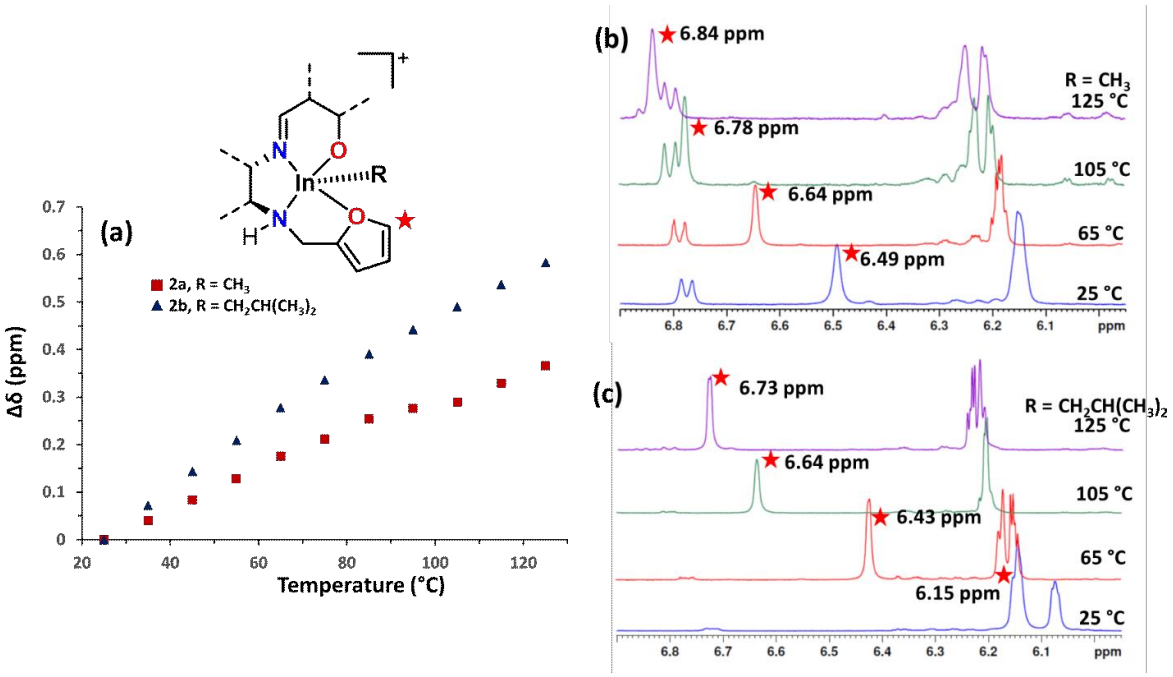

Figure 6. a) Downfield shift of the α proton of the furfuryl pendant arm relative to 25 °C. VT ^{1}H NMR (400 MHz, C_6D_5Br, 25–125 °C) spectra showing downfield migration of the α proton of the furfuryl group of **2a** (b) and **2b** (c).

Substrate coordination to the indium center and product formation can follow several possible pathways (Figure 7). In scenario A, epoxide coordinates first to the catalyst and the insertion of **ε-CL** or epoxide into a coordinated epoxide results in either **SOE** or polyether respectively (Figure 7 A1-2). Alternatively, **ε-CL** coordinates first and the insertion of epoxide or **ε-CL** into a coordinated **ε-CL** results in a cyclic ether-ester compound or polycaprolactone (Figure 7B1-2 and Figure S61). However, of these pathways, only the product from path A2, **SOE**, is observed. While epoxides or **ε-CL** can be homopolymerized by cationic indium complexes at higher temperatures and concentrations,[26,31,50] these polymerizations do not occur under the current reaction conditions due to the relatively low Lewis acidity of the catalyst. The relative Lewis acidity of **2b**, determined by a modified Gutmann-Becket method,[51-53] is significantly lower than that of compounds such as BF_3 (Figure1a) that can homopolymerize both **ε-CL** and epoxide under the reaction conditions used herein (δ = 78.2 ppm for BF_3 and δ = 69.4 ppm for **2b** in the $^{31}P\{^1H\}$ NMR spectrum, see SI).[27]

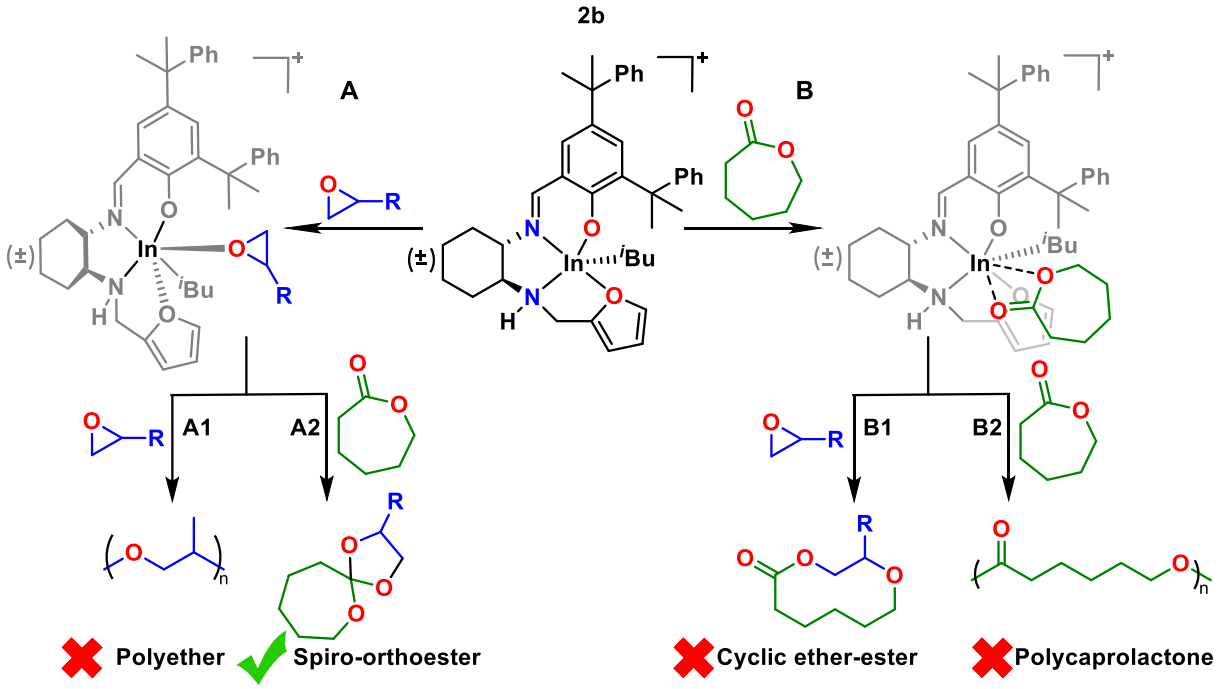

Figure 7. Possible pathways for substrate coordination and product formation by **2b**.

The first step in our proposed mechanism is the coordination of an epoxide to the cationic center, as neither homopolymerization products nor a cyclic ether-ester species is observed. We used triethylphosphine oxide (TEPO) as a non-reactive model for epoxide coordination in order to probe the impact of catalyst reactivity with either one or two coordinated epoxide molecules using a modified Gutmann-Beckett method (Figure 8).[51-53] The $^{31}P\{^{1}H\}$ NMR spectrum of **2b** mixed with 1 equivalent of TEPO (**2b**•TEPO) shows a broad signal at δ = 69.4 ppm. The broadness of this peak arises from the fluxional behavior of the furfuryl pendant arm at 25 °C resulting in the reversible association and dissociation of the TEPO molecule (Figures 8a, S55, S56). Conversely, when two equivalents of TEPO are mixed with **2b** the resulting $^{31}P\{^{1}H\}$ NMR spectrum shows a single sharp peak at δ = 59.6 ppm (Figures 8b, S55, S56). While both species show a downfield shift of the TEPO $^{31}P\{^{1}H\}$ peak compared to free TEPO (δ = 45.8 ppm), **2b**•TEPO is more Lewis acidic than **2b**•2TEPO and thus expected to be the more reactive species.[51,52]

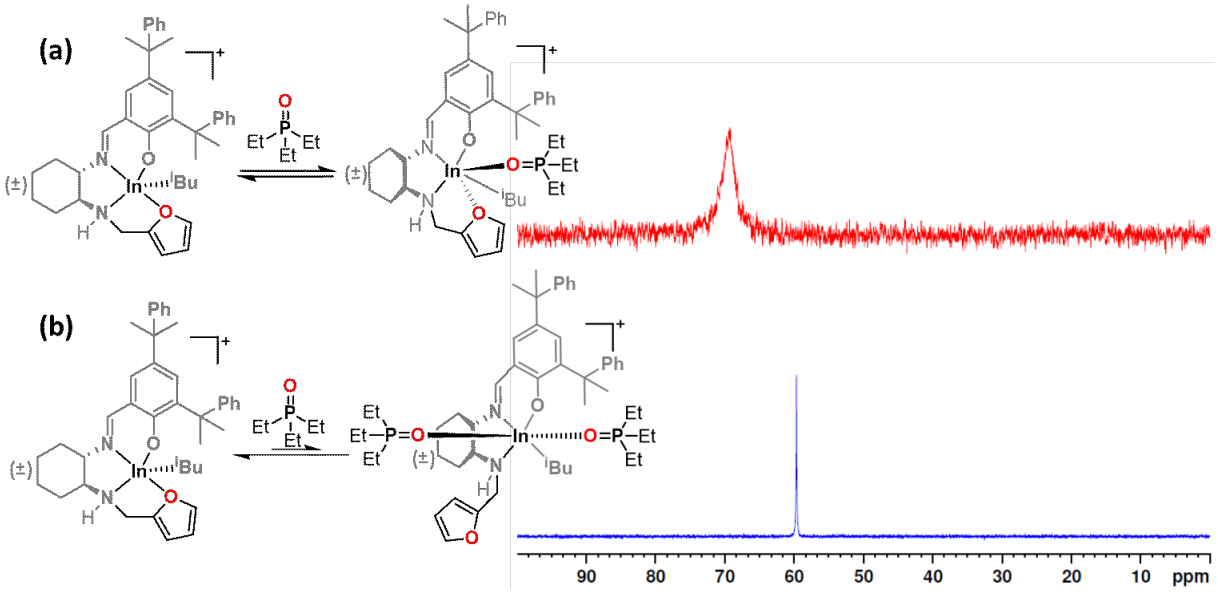

Figure 8. (a) Broad $^{31}P\{^{1}H\}$ NMR peak arising from the coordination of one TEPO molecule to **2b** and (b) sharp $^{31}P\{^{1}H\}$ NMR peak from the coordination of two TEPO molecules to **2b**. ($^{31}P\{^{1}H\}$ NMR 162 MHz, 25 °C, Tol-d_8).

Additionally, computational studies show that the mono-epoxide species is more stable (~7 kcal mol^{-1}) than the bis-epoxide in benzene, where the coordination of two epoxide molecules leads to the complete dissociation of the pendant furan (Figure S62). Thus, coordination of one epoxide leads to a more stable and more active catalyst. Based on these studies, spiro-orthoester formation is preceded by the coordination of a single epoxide molecule resulting in the active catalytic species.

Computational studies. The first step of the proposed mechanism involves the S_N2 attack of the epoxide by lactone and subsequent ring opening of the epoxide (Scheme 2A). This attack can occur at either carbon of the epoxide, resulting in two possible isomers. The subsequent steps of the cycle involve ring closing, release of the product, and regeneration of the active catalyst (Scheme 2B).

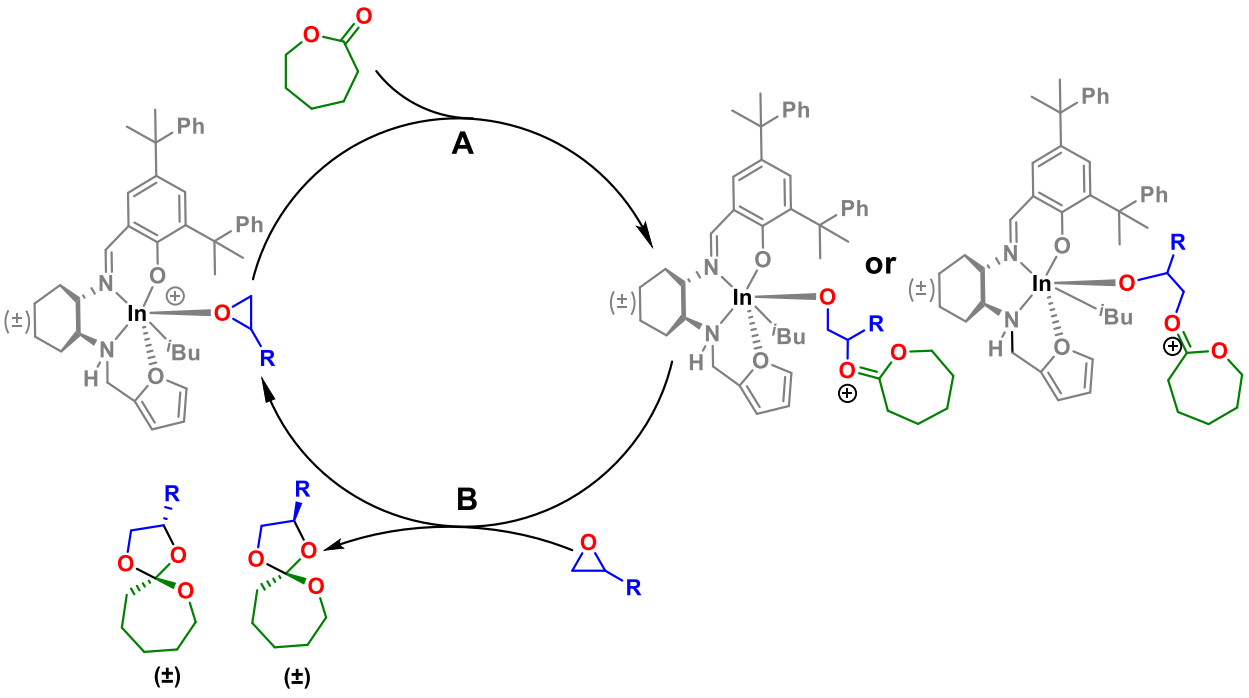

Scheme 2. Proposed mechanism for spiro-orthoester formation by **2b**.

We used computational methods to gain further insight into the mechanism since the Michaelis-Menten saturation kinetics makes it considerably difficult to study the the proposed mechanism experimentally. These calculations were performed with a truncated **2a** (methyl groups instead of

Me_2PhC) as a model and 1,2-epoxybutane as a simplified epoxide (Figure 9). Although all four possible stereoisomers are observed experimentally, only the pathway for the formation of one stereoisomer was examined for brevity.

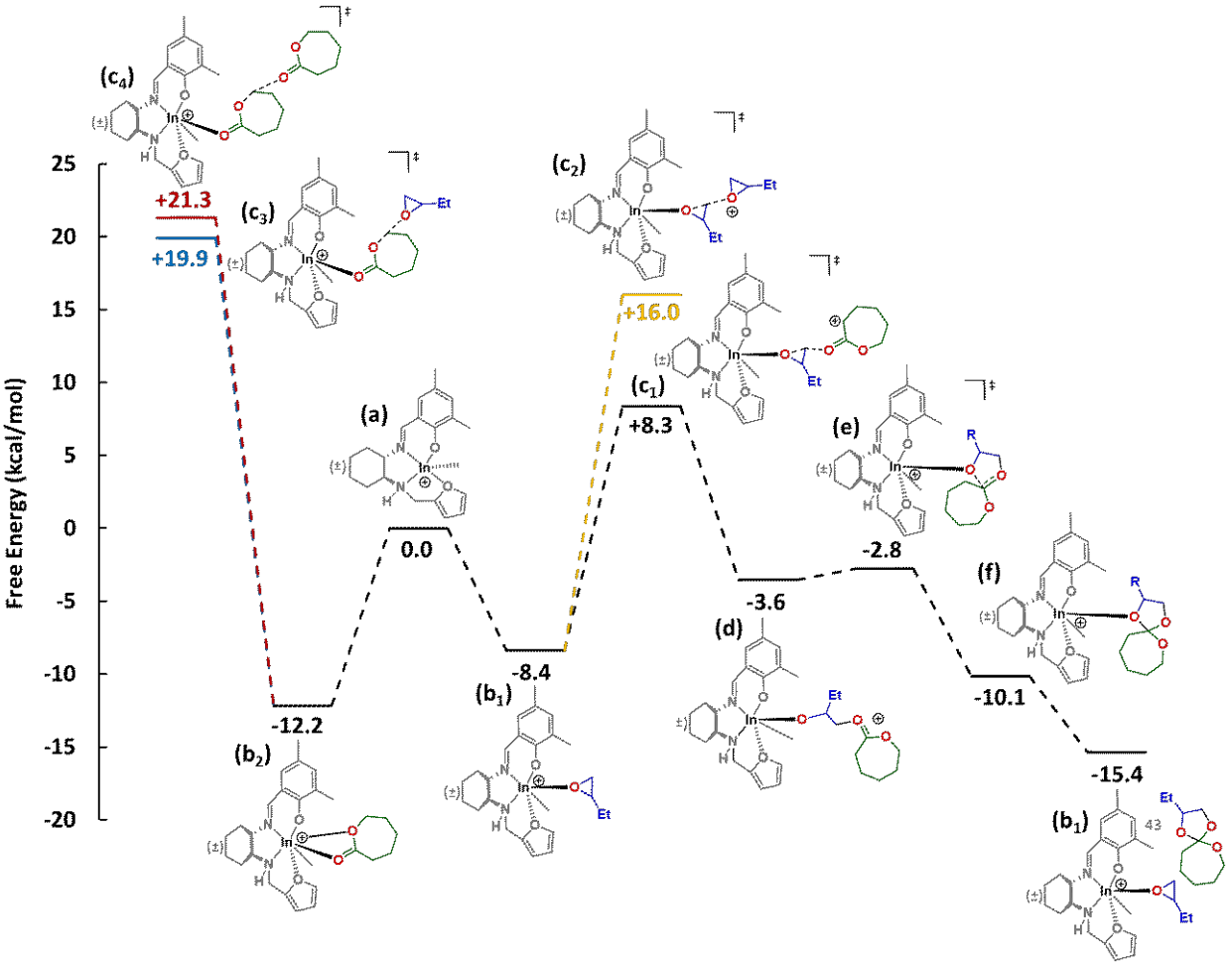

Figure 9. Proposed reaction profile for **SOE** formation by a truncated model of **2a**.

When **ε-CL** and epoxide are present, either one can coordinate to the indium center. In the case of **ε-CL** coordination, either an epoxide or an additional **ε-CL** can ring open the coordinated

lactone molecule (Figure 9, c_3 and c_4, respectively). However, the kinetic barriers for both these scenarios are considerably higher than that of **ε-CL** attacking a coordinated epoxide (Figure 9, c_1), consistent with the fact that the homo-polymerizations of **ε-CL** and of the epoxide do not occur. Based on these calculations, the rate determining step (+16.7 kcal mol^{-1}, Figure 9, c_1) is the S_N2 attack on and the simultaneous ring opening of the coordinated epoxide by **ε-CL**, resulting in the formation of a new indium alkoxy bond (Figure 9d).

The last step of the cycle is the attack on the carbonyl carbon of **ε- CL** by the indium alkoxide oxygen and the formation of the spiro-orthoester. This is followed by the release of the newly formed spiro-orthoester and regeneration of the active catalyst upon the coordination of a new epoxide molecule.

The steric bulk of the alkyl species has a significant impact on this step of the reaction. $\%V_{bur}$ calculations of the catalyst coordinated to SOE show that the steric environment is different between **2a** and **2b** or **2c** (Figure 10), contributing to **2b** and **2c** reaching higher conversions.

R =	CH_3	$CH_2CH(CH_3)_2$	$CH_2Si(CH_3)_3$
% Free Volume	12.5	5.7	4.7
% Buried Volume	87.5	94.3	95.3

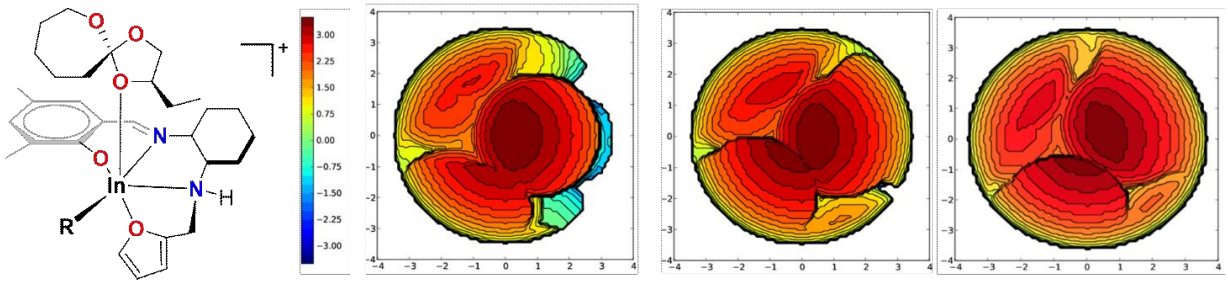

Figure 10. $\%V_{bur}$ (at a 3.5 Å radius around the indium center) calculation to determine steric bulk of different alkyl ligands on **2a-SOE**, **2b-SOE**, and **2c-SOE**.

Conclusions

We investigated the mechanism of the spiro-orthoester synthesis through the coupling of epoxides and ε-caprolactone. We used model catalysts with different In-alkyl and substituted furfuryl pendant ligands to probe the structure function relationships in reactivity and mechanism. We found out that increased steric bulk and weak electron donation of the alkyl ligands increase the rate of reaction.

The main question in this study was to determine why these catalysts, in the presence of lactones and epoxides, form spiro-orthoesters exclusively *in lieu* of a mixture of **SOE**, polyether, and polyesters. We found out that these catalysts follow Michaelis-Menten type saturation kinetics, with the reaction being zeroth order with respect to both substrates and first order with respect to catalyst, with a Michaelis constant comparable to a slow reacting enzyme. Concurrently, the limited Lewis acidity of these systems under these reaction conditions prevents the homo-polymerization of epoxides or ε-caprolactone. Finally, we show using DFT calculations that the reaction proceeds through the coordination of one epoxide molecule to the cationic indium center followed by the coupling to a lactone molecule resulting in the selective formation of spiro-orthoesters.

ASSOCIATED CONTENT

Supporting Information

The Supporting Information is available free of charge on the ACS Publications website.

[Experimental section, characterization of metal complexes in solution and in the solid state]

AUTHOR INFORMATION

Corresponding Authors

Parisa Mehrkhodavandi (mehr@chem.ubc.ca), Paula L. Diaconescu (pld@chem.ucla.edu)

Author Contributions

The manuscript was written through contributions of all authors. All authors have given approval to the final version of the manuscript. ‡These authors contributed equally.

ACKNOWLEDGMENT

The authors acknowledge support from the Natural Sciences and Engineering Council (NSERC) of Canada. The computational studies were supported by the NSF (Grant CHE-1809116 to PLD).

REFERENCES

1. Jia, Z. W.; Jiang, J. X.; Zhang, X. F.; Cui, Y. Q.; Chen, Z. C.; Pan, X. B.; Wu, J. C., Isotactic-Alternating, Heterotactic-Alternating, and ABAA-Type Sequence-Controlled Copolyester Syntheses via Highly Stereoselective and Regioselective Ring-Opening Polymerization of Cyclic Diesters. *J. Am. Chem. Soc.* **2021**, *143*, 4421-4432, 10.1021/jacs.1c00902.
2. Li, J.; Stayshich, R. M.; Meyer, T. Y., Exploiting Sequence To Control the Hydrolysis Behavior of Biodegradable PLGA Copolymers. *J. Am. Chem. Soc.* **2011**, *133*, 6910-6913, 10.1021/ja200895s.
3. Mochizuki, S.; Ogiwara, N.; Takayanagi, M.; Nagaoka, M.; Kitagawa, S.; Uemura, T., Sequence-regulated copolymerization based on periodic covalent positioning of monomers along one-dimensional nanochannels. *Nat. Commun.* **2018**, *9*, 10.1038/s41467-017-02736-1.
4. Xia, X.; Suzuki, R.; Gao, T.; Isono, T.; Satoh, T., One-step synthesis of sequence-controlled multiblock polymers with up to 11 segments from monomer mixture. *Nat. Commun.* **2022**, *13*, 10.1038/s41467-021-27830-3.
5. Amy, L.; Zachary, C. H.; Yi, S.; Ruxi, D.; Paula, L. D., 9.07 - Metal Complexes for Redox Switching and Control of Reactivity. In *Comprehensive Coordination Chemistry III*, Edwin C. Constable, G. P., Lawrence Que Jr, Ed. Elsevier: 2021; pp 155-180, https://doi.org/10.1016/B978-0-08-102688-5.00044-1.
6. Chung, K.; Takata, T.; Endo, T., Anionic Ring-Opening Copolymerization of Bicyclic Bis(.gamma.-lactone)s with Mono- and Bifunctional Epoxides via Double Ring-Opening Isomerization of the Bis(.gamma.-lactone)s and Volume Change during Copolymerization. *Macromolecules* **1995**, *28*, 3048-3054, 10.1021/ma00113a006.
7. Uenishi, K.; Sudo, A.; Endo, T., Anionic alternating copolymerization of 3,4- dihydrocoumarin and glycidyl ethers: A mew approach to myester synthesis. *J. Polym. Sci. Pol. Chem.* **2008**, *46*, 4092-4102, 10.1002/pola.22752.

8. Uenishi, K.; Sudo, A.; Endo, T., Anionic Alternating Copolymerization Behavior of Bifunctional Six-Membered Lactone and Glycidyl Phenyl Ether. *J. Polym. Sci. Pol. Chem.* **2009**, *47*, 3662-3668, 10.1002/pola.23446.
9. Uenishi, K.; Sudo, A.; Endo, T., Anionic Alternating Copolymerization of a Bifunctional Six-Membered Lactone and Glycidyl Phenyl Ether: Selective Synthesis of a Linear Polyester Having Lactone Moiety. *J. Polym. Sci. Pol. Chem.* **2009**, *47*, 1661-1672, 10.1002/pola.23263.
10. Uenishi, K.; Sudo, A.; Endo, T., Synthesis of Polyester Having Sequentially Ordered Two Orthogonal Reactive Groups by Anionic Alternating Copolymerization of Epoxide and Bislactone. *J. Polym. Sci. Pol. Chem.* **2009**, *47*, 6750-6757, 10.1002/pola.23714.
11. Van Zee, N. J.; Coates, G. W., Alternating copolymerization of dihydrocoumarin and epoxides catalyzed by chromium salen complexes: a new route to functional polyesters. *Chem. Commun.* **2014**, *50*, 6322-6325, 10.1039/c4cc01566e.
12. Nishimori, K.; Ouchi, M., AB-alternating copolymers via chain-growth polymerization: synthesis, characterization, self-assembly, and functions. *Chem. Commun.* **2020**, *56*, 3473-3483, 10.1039/d0cc00275e.
13. Qu, C. K.; Li, Z. H.; He, J. P., Synthesis of copolymers with an exact alternating sequence using the cationic polymerization of pre-sequenced monomers. *Polym. Chem.* **2018**, *9*, 3455- 3460, 10.1039/c8py00626a.
14. Zhao, W. C.; Li, F. K.; Li, C. K.; He, J. H.; Zhang, Y. T.; Chen, C. L., Lewis Pair Catalyzed Regioselective Polymerization of (E,E)-Alkyl Sorbates for the Synthesis of (AB)(n) Sequenced Polymers. *Angew. Chem. Int. Ed.* **2021**, *60*, 24306-24311, 10.1002/anie.202111336.
15. Zhou, P.; Takaishi, Y.; Duan, H. Q.; Chen, B.; Honda, G.; Itoh, M.; Takeda, Y.; Kodzhimatov, O. K.; Lee, K. H., Coumarins and bicoumarin from Ferula sumbul: anti-HIV activity and inhibition of cytokine release. *Phytochemistry* **2000**, *53*, 689-697, 10.1016/s0031- 9422(99)00554-3.
16. Ohta, T.; Maruyama, T.; Nagahashi, M.; Miyamoto, Y.; Hosoi, S.; Kiuchi, F.; Yamazoe, Y.; Tsukamoto, S., Paradisin C: a new CYP3A4 inhibitor from grapefruit juice. *Tetrahedron* **2002**, *58*, 6631-6635, 10.1016/s0040-4020(02)00739-1.
17. Taniguchi, M.; Xiao, Y. Q.; Liu, X. H.; Yabu, A.; Hada, Y.; Guo, L. Q.; Yamazoe, Y.; Baba, K., Rivulobirin E and rivulotririn C from Pleurospermum rivulorum. *Chem. Pharm. Bull.* **1999**, *47*, 713-715,
18. Bodenbenner, K., Uber spirocyclische orthoester. *Justus Liebigs Ann. Chem.* **1959**, *623*, 183-191,
19. Yokozawa, T.; Sato, M.; Endo, T., Preparation and polymerization of spiroorthoester bearing the perfluoroalkyl group. *J. Polym. Sci. Pol. Chem.* **1990**, *28*, 1841-1846, 10.1002/pola.1990.080280716.
20. Nishida, H.; Sanda, F.; Endo, T.; Nakahara, T.; Ogata, T.; Kusumoto, K., Polyaddition of bifunctional spiro orthoesters with bifunctional acid chlorides accompanying double ring- opening isomerization. *J. Polym. Sci. Pol. Chem.* **2000**, *38*, 68-73, 10.1002/(sici)1099-0518(20000101)38:1<68::aid-pola9>3.3.co;2-w.
21. Chikaoka, S.; Takata, T.; Endo, T., Synthesis and reactions of exo-methylene-containing poly(cyclic orthoester). *Macromolecules* **1994**, *27*, 2380-2382, 10.1021/ma00087a003.
22. Chikaoka, S.; Takata, T.; Endo, T., Cationic ring-opening polymerization of spiroorthoester: polymer structure, polymerization mechanism, and volume change on polymerization. *Macromolecules* **1992**, *25*, 625-628, 10.1021/ma00028a022.

23. Lombard, F. J.; Lepage, R. J.; Schwartz, B. D.; Johnston, R. C.; Healy, P. C.; Krenske, E. H.; Coster, M. J., Synthesis of spirocyclic orthoesters by 'anomalous' rhodium(II)-catalysed intramolecular C-H insertions. *Org. Biomol. Chem.* **2018**, *16*, 256-261, 10.1039/c7ob02123b.
24. Tortoreto, C.; Achard, T.; Egger, L.; Guenee, L.; Lacour, J., Synthesis of Spiro Ketals, Orthoesters, and Orthocarbonates by CpRu-Catalyzed Decomposition of alpha-Diazo-beta-ketoesters. *Org. Lett.* **2016**, *18*, 240-243, 10.1021/acs.orglett.5b03380.
25. Chabanne, P.; Tighzert, L.; Pascault, J. P., Monoepoxy polymerization initiated by BF(3)-amine complexes in bulk. 3. Influence of gamma-butyrolactone on polymer formation. *J. Appl. Polym. Sci.* **1994**, *53*, 787-806, 10.1002/app.1994.070530608.
26. Jung, H. J.; Chang, C.; Yu, I.; Aluthge, D. C.; Ebrahimi, T.; Mehrkhodavandi, P., Coupling of Epoxides and Lactones by Cationic Indium Catalysts To Form Functionalized Spiro- Orthoesters. *ChemCatChem* **2018**, *10*, 3219-3222, 10.1002/cctc.201800474.
27. Jung, H. J.; Goonesinghe, C.; Mehrkhodavandi, P., Temperature triggered alternating copolymerization of epoxides and lactones via pre-sequenced spiroorthoester intermediates. *Chem. Sci.* **2022**, *13*, 3713-3718, 10.1039/d1sc06634j.
28. Diaz, C.; Tomkovic, T.; Goonesinghe, C.; Hatzikiriakos, S. G.; Mehrkhodavandi, P., One- Pot Synthesis of Oxygenated Block Copolymers by Polymerization of Epoxides and Lactide Using Cationic Indium Complexes. *Macromolecules* **2020**, *53*, 8819-8828, 10.1021/acs.macromol.0c01276.
29. Goonesinghe, C.; Jung, H. J.; Roshandel, H.; Diaz, C.; Baalbaki, H. A.; Nyamayaro, K.; Ezhova, M.; Hosseini, K.; Mehrkhodavandi, P., An Air Stable Cationic Indium Catalyst for Formation of High-Molecular-Weight Cyclic Poly(lactic acid). *ACS Catal.* **2022**, *12*, 7677−7686, 10.1021/acscatal.2c02118.
30. Baalbaki, H. A.; Nyamayaro, K.; Shu, J. L.; Goonesinghe, C.; Jung, H. J.; Mehrkhodavandi, P., Indium-Catalyzed CO2/Epoxide Copolymerization: Enhancing Reactivity with a Hemilabile Phosphine Donor. *Inorg. Chem.* **2021**, *60*, 19304-19314, 10.1021/acs.inorgchem.1c03123.
31. Goonesinghe, C.; Roshandel, H.; Diaz, C.; Jung, H. J.; Nyamayaro, K.; Ezhova, M.; Mehrkhodavandi, P., Cationic indium catalysts for ring opening polymerization: tuning reactivity with hemilabile ligands. *Chem. Sci.* **2020**, *11*, 6485-6491, 10.1039/d0sc01291b.
32. Garcia-Garcia, A.; Serna, S.; Yang, Z.; Delso, I.; Taleb, V.; Hicks, T.; Artschwager, R.; Vakhrushev, S. Y.; Clausen, H.; Angulo, J.; Corzana, F.; Reichardt, N. C.; Hurtado-Guerrero, R., FUT8-Directed Core Fucosylation of N-glycans Is Regulated by the Glycan Structure and Protein Environment. *ACS Catal.* **2021**, *11*, 9052-9065, 10.1021/acscatal.1c01698.
33. Calzadiaz-Ramirez, L.; Calvo-Tusell, C.; Stoffel, G. M. M.; Lindner, S. N.; Osuna, S.; Erb, T. J.; Garcia-Borras, M.; Bar-Even, A.; Acevedo-Rocha, C. G., In Vivo Selection for Formate Dehydrogenases with High Efficiency and Specificity toward NADP(+). *ACS Catal.* **2020**, *10*, 7512-7525, 10.1021/acscatal.0c01487.
34. Mahdavi-Shakib, A.; Sempel, J.; Babb, L.; Oza, A.; Hoffman, M.; Whittaker, T. N.; Chandler, B. D.; Austin, R. N., Combining Benzyl Alcohol Oxidation Saturation Kinetics and Hammett Studies as Mechanistic Tools for Examining Supported Metal Catalysts. *ACS Catal.* **2020**, *10*, 10207-10215, 10.1021/acscatal.0c02212.
35. Liu, S. B., Where does the electron go? The nature of ortho/para and meta group directing in electrophilic aromatic substitution. *J. Chem. Phys.* **2014**, *141*, 10.1063/1.4901898.
36. Liu, S. B., Quantifying Reactivity for Electrophilic Aromatic Substitution Reactions with Hirshfeld Charge. *J. Phys. Chem. A* **2015**, *119*, 3107-3111, 10.1021/acs.jpca.5b00443.

37. Chernyshov, I. Y.; Ananyev, I. V.; Pidko, E. A., Revisiting van der Waals Radii: From Comprehensive Structural Analysis to Knowledge-Based Classification of Interatomic Contacts. *ChemPhysChem* **2020**, *21*, 370-376, 10.1002/cphc.201901083.
38. Bondi, A., Van der Waals Volumes + radii. *J. Phys. Chem.* **1964**, *68*, 441-442, 10.1021/j100785a001.
39. Bures, J., A Simple Graphical Method to Determine the Order in Catalyst. *Angew. Chem. Int. Ed.* **2016**, *55*, 2028-2031, 10.1002/anie.201508983.
40. Bures, J., Variable Time Normalization Analysis: General Graphical Elucidation of Reaction Orders from Concentration Profiles. *Angew. Chem. Int. Ed.* **2016**, *55*, 16084-16087, 10.1002/anie.201609757.
41. Roskoski, R., Michaelis-Menten Kinetics. In *Reference Module in Biomedical Sciences*, Elsevier: 2015, https://doi.org/10.1016/B978-0-12-801238-3.05143-6.
42. Wijeratne, G. B.; Corzine, B.; Day, V. W.; Jackson, T. A., Saturation Kinetics in Phenolic O-H Bond Oxidation by a Mononuclear Mn(III)-OH Complex Derived from Dioxygen. *Inorg. Chem.* **2014**, *53*, 7622-7634, 10.1021/ic500943k.
43. Northrop, D. B., On the Meaning of Km and V/K in Enzyme Kinetics. *J. Chem. Ed.* **1998**, *75*, 1153, 10.1021/ed075p1153.
44. Bar-Even, A.; Noor, E.; Savir, Y.; Liebermeister, W.; Davidi, D.; Tawfik, D. S.; Milo, R., The Moderately Efficient Enzyme: Evolutionary and Physicochemical Trends Shaping Enzyme Parameters. *Biochemistry* **2011**, *50*, 4402-4410, 10.1021/bi2002289.
45. Pirrung, M. C.; Liu, H.; Morehead, A. T., Rhodium Chemzymes: Michaelis−Menten Kinetics in Dirhodium(II) Carboxylate-Catalyzed Carbenoid Reactions. *J. Am. Chem. Soc.* **2002**, *124*, 1014-1023, 10.1021/ja011599l.
46. Miyanaga, K.; Unno, H., 2.05 - Reaction Kinetics and Stoichiometry. In *Comprehensive Biotechnology (Second Edition)*, Moo-Young, M., Ed. Academic Press: Burlington, 2011; pp 33- 46, https://doi.org/10.1016/B978-0-08-088504-9.00085-4.
47. Falivene, L.; Cao, Z.; Petta, A.; Serra, L.; Poater, A.; Oliva, R.; Scarano, V.; Cavallo, L., Towards the online computer-aided design of catalytic pockets. *Nat. Chem.* **2019**, *11*, 872-879, 10.1038/s41557-019-0319-5.
48. Thorley, K. J.; Benford, M.; Song, Y.; Parkin, S. R.; Risko, C.; Anthony, J. E., What is special about silicon in functionalised organic semiconductors? *Mater. Adv.* **2021**, *2*, 5415-5421, 10.1039/d1ma00447f.
49. Bassindale, A. R.; Glynn, S. J.; Taylor, P. G., Activating and Directive Effects of Silicon. In *PATAI'S Chemistry of Functional Groups*, Rappoport, Z.; Apeloig, Y., Eds. 1998; pp 355-430,
50. Diaz, C.; Ebrahimi, T.; Mehrkhodavandi, P., Cationic indium complexes for the copolymerization of functionalized epoxides with cyclic ethers and lactide. *Chem. Commun.* **2019**, *55*, 3347-3350, 10.1039/c8cc08858f.
51. Mayer, U.; Gutmann, V.; Gerger, W., The acceptor number — A quantitative empirical parameter for the electrophilic properties of solvents. *Monatsh. Chem.* **1975**, *106*, 1235-1257, 10.1007/BF00913599.
52. Welch, G. C.; Cabrera, L.; Chase, P. A.; Hollink, E.; Masuda, J. D.; Wei, P. R.; Stephan, D. W., Tuning Lewis acidity using the reactivity of "frustrated Lewis pairs": facile formation of phosphine-boranes and cationic phosphonium-boranes. *Dalton Trans.* **2007**, 3407-3414, 10.1039/b704417h.
53. Beckett, M. A.; Strickland, G. C.; Holland, J. R.; Varma, K. S., A convenient NMR method for the measurement of Lewis acidity at boron centres: Correlation of reaction rates of Lewis

acid initiated epoxide polymerizations with Lewis acidity. *Polymer* **1996**, *37*, 4629-4631, 10.1016/0032-3861(96)00323-0.